

Quasi-Electrostatic Simulation of Energy Density Limits and Variability in Nanoparticle Composite Materials

B. Costello⁽¹⁾⁽²⁾, J. A. Davis⁽¹⁾⁽³⁾

⁽¹⁾ Georgia Institute of Technology, Atlanta, GA, USA
⁽²⁾ bcostello3@gatech.edu ⁽³⁾ jeff.davis@ece.gatech.edu

ABSTRACT

To understand the limits and opportunities of nanoparticle (NP) composite materials, it is imperative to better understand the heterogeneous electric field distributions within such materials. Using a custom-built simulator, the electric field is simulated and used to compute the effective permittivity, breakdown field strength, and maximum energy density for over 1500 randomly generated NP geometries. The parameters of the geometries simulated in this work are modeled after measured composites, and are used for verification [1]. In addition, the variability of key electrical parameters is characterized, and the microstructure of the simulated composite is categorized as percolating, near-percolating, or non-percolating. Initial conclusions of this analysis reveal that the highest energy density samples have a non-percolating configuration in a volume fraction range from 20% to 40%. These geometries exhibit up to a 14% increase in energy density compared to a pure Polyvinylidene Fluoride (PVDF) sample.

Keywords: Simulation, Energy Storage, Capacitors, Nanoparticles, Composite Materials

1 INTRODUCTION

A 3-D quasi-electrostatic and material composition simulator has been developed which generates random material geometries of nanocomposite materials. Specifically, these simulated microstructures are used to model state-of-the-art, solid-state capacitive energy storage devices that are com-

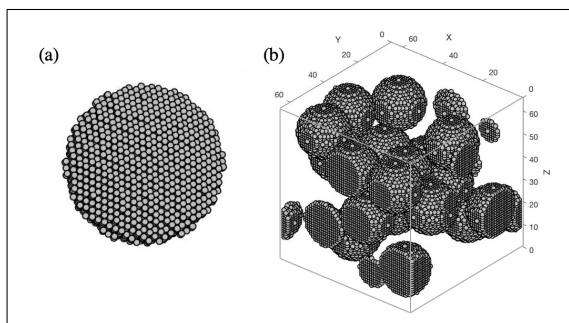


Figure 1: Representation of (a) a single nanoparticle in a finite difference grid and (b) a stochastically generated 3-D geometry at a volume fraction of 0.25.

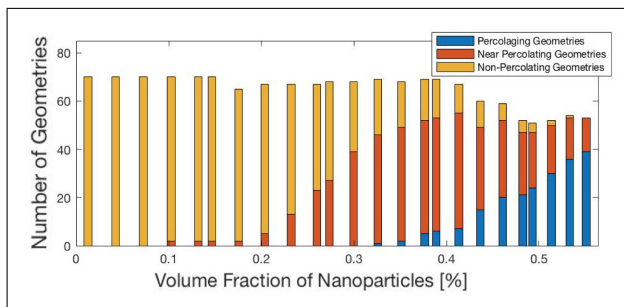


Figure 2: Histogram of simulated microstructures classified by percolating behavior of NP at each volume fraction.

posed of dielectric nanoparticles (e.g. BaTiO_3) embedded in a high dielectric strength polymer matrix (e.g. PVDF) [1]. The data reported in this paper includes a large set of microstructures that are simulated using the resources at the Partnership for Advanced Computing Environment (PACE) computing cluster at the Georgia Institute of Technology.

The NP diameter (40nm) and material composition (i.e. BaTiO_3 and PVDF) of the samples explored in this paper are consistent with the fabricated composite materials in [1]. Over 1500 simulated composite geometries with nanoparticle inclusions are generated and subsequently analyzed by the material simulator at varying volume percentages ranging from 0 to 60%, in increments of 2.5%. Currently, this simulator analyzes the electrical properties of each simulated geometry at various applied DC voltages, which is appropriate for energy storage devices that operate by definition at low frequencies. In addition, a large sample set of unique microstructures are simulated so that the variability of the effective dielectric constant and the effective dielectric strength is characterized in this analysis. These results illustrate how random differences in microstructure translate into changes in key electrical properties of the composites. As seen in Figure 2, a salient attribute of NP connectivity is also tracked throughout this analysis. This attribute describes whether the NPs of a simulated geometry are in a non-percolating, near-percolating, or fully-percolating configuration.

2 SIMULATOR DESCRIPTION

To generate a large number of datasets, a custom simulator was built. The functionality of this simulator can be broken down into three parts: material generation, material

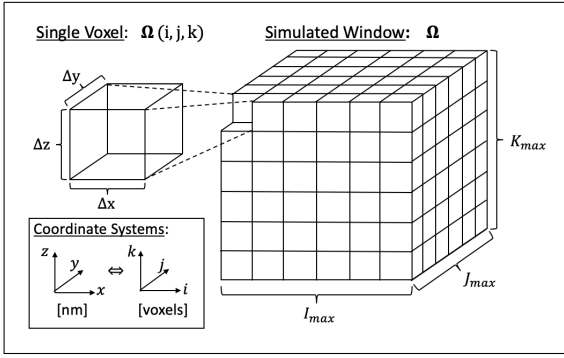


Figure 3: Illustration of simulated space including a depiction of critical dimensional parameters and the correspondence between discrete indices (i, j, k) and cartesian coordinates (x, y, z) .

characterization, and material analysis. This simulator requires a user-defined set of input parameters, which includes window size, NP diameter, NP volume fraction, and several material parameters.

The first stage of this simulation platform is material generation. Based on the volume fraction and nanoparticle size, an estimate for the number of nanoparticles is determined. Using this estimate, the simulator populates the simulated window with nanoparticle locations, making sure that NP spheres do not intersect more than a few voxels. In the case that a nanoparticle is placed on the edge of the simulated window, a second nanoparticle on the opposite side of the simulated window is created to maintain circular boundary conditions and, therefore, material continuity. The nanoparticle locations and radii $(x, y, z, \text{ and } r)$ are stored in rows of a matrix and subsequently used to populate the voxels of the simulated window.

After constructing the geometry in its explicit voxelated form, the second stage of this simulation platform uses a control volume technique to solve the 3-D Laplace equation. Two Dirichlet boundary conditions are applied to the top and bottom of the simulated window. The transformation matrix (\mathbf{A}) and boundary vector (\hat{b}) were constructed using a finite difference method. Periodic boundary conditions in the \hat{x} and \hat{y} directions maintain continuity along the fringes of the simulated space. The electrostatic potential at each discrete point (\hat{v}) is computed by solving the following matrix.

$$\mathbf{A}\hat{v} = \hat{b} \quad (1)$$

This results in an approximation of the electrostatic potential, which is then used to compute the 3-D electric field by taking the negative gradient of the electrostatic potential through the entire simulated window.

$$\vec{\mathbf{E}}(x, y, z) = -\nabla V(x, y, z) \quad (2)$$

The magnitude of this electric field $(|\vec{\mathbf{E}}|)$ at each voxel is then used to compute the energy density at one volt (E_d) , effective composite permittivity (ϵ_{eff}) , effective composite

breakdown field strength (E_{BD}) , and maximum energy density $(E_{d_{max}})$. In order to calculate these composite material properties, the energy density is computed by calculating the total energy stored in the electric fields (E_{total}) .

$$E_{total} = \sum_{i=1}^{I_{max}} \sum_{j=1}^{J_{max}} \sum_{k=1}^{K_{max}} \left[\frac{1}{2} \epsilon_0 \epsilon_{ijk} |\vec{\mathbf{E}}_{ijk}|^2 \Delta x \Delta y \Delta z \right] \quad (3)$$

$$E_d = \frac{E_{total}}{(\Delta x I_{max})(\Delta y J_{max})(\Delta z K_{max})} \quad (4)$$

The capacitance is found and subsequently used to compute the effective relative permittivity of the composite.

$$C = \frac{2E_{total}}{V_{app}^2} = \epsilon_{eff} \frac{\epsilon_0 A}{d} \quad (5)$$

$$\epsilon_{eff} = \frac{2E_{total}(\Delta z K_{max})}{V_{app}^2 \epsilon_0 (\Delta x I_{max})(\Delta y J_{max})} \quad (6)$$

In an effort to quantify the limits of energy density in these simulated composites, the breakdown voltage is approximated by (7), which leverages the fact that the applied simulation voltage (V_{app}) is used to determine a non-dimensional scaling factor which represents the theoretical maximum voltage (V_{max}) . This is consistent with the analysis in [2].

$$V_{max(host)} = (V_{app}) \frac{E_{bd(host)}}{((\mathbf{E}_j)_{(host)} + \sigma_{E(host)})|_{V_{app}}} \quad (7)$$

This equation can be used to calculate the maximum voltage exclusively in either the host material or the nanoparticle material. To determine the actual maximum voltage of the simulated device, the minimum of these two voltages is chosen to represent the breakdown of the simulated device. The breakdown voltage is then used to determine the maximum theoretical energy density. This approach aims to more accurately predict the breakdown field strength in multi-phase composite materials at higher volume fractions because it takes into account both the host and NP breakdown properties.

3 MODEL & SIMULATOR VALIDATION

After ensuring that the simulation produces the correct electric field values for simplest-case geometries, initial validation was carried out. To do this, simulated values of the effective permittivity and effective breakdown field strength (i.e. breakdown voltage divided by composite sample thickness) are compared to measurements reported in [1]. For these preliminary simulations a voxel size of $2.5\text{nm} \times 2.5\text{nm} \times 2.5\text{nm}$ and a simulation window size of 65 voxels in each direction (x, y, z) is used. The BaTiO_3 nanoparticles are roughly 40nm in diameter. As seen in Figure 4, the effective permittivity is computed and compared both to the classical Bruggeman's equation and the data reported in [1]. The values of

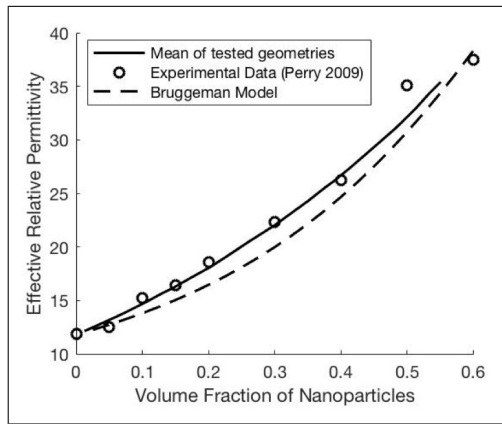


Figure 4: Comparison of average simulation results to measured data for the effective permittivity of composites [1].

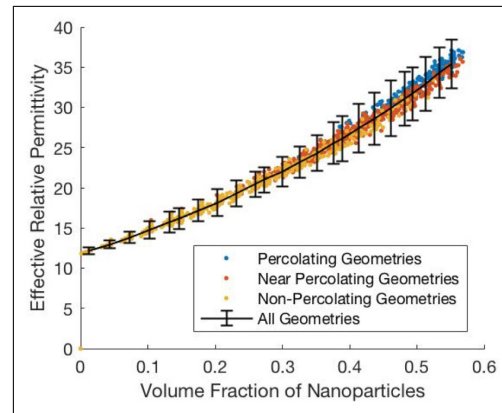


Figure 6: Scatter plot of effective permittivity showing the range of variability among 1500 simulated material microstructures.

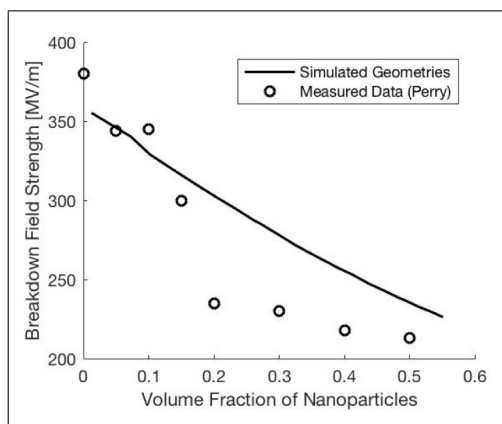


Figure 5: Comparison of average simulation results to measured data for the effective breakdown field strength of composites [1].

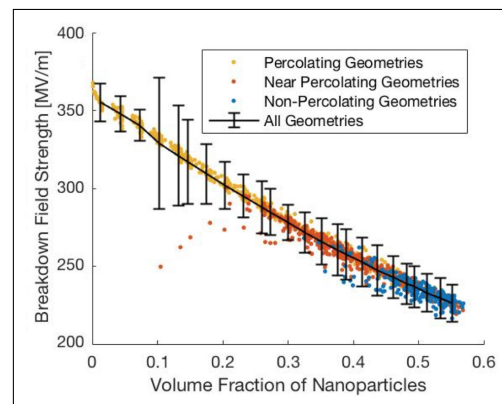


Figure 7: Scatter plot of effective breakdown field strength (i.e. breakdown voltage divided by sample thickness) showing the range of variability among 1500 simulated material microstructures.

dielectric permittivity used for the BaTiO₃ nanoparticles ($\epsilon_r = 80$) and PVDF matrix ($\epsilon_r = 11.9$) is taken from [1]. The breakdown model is also compared to published data in [1] in Figure 5. Both data sets provide preliminary validation of the simulator's ability to predict the quantities that are used to measure energy density limits.

4 VARIABILITY OF PARAMETERS

One major contribution of this research effort is the ability to explore and better understand the variability of electrical properties among these state-of-the-art nanocomposite materials. The material generation component of this simulator is based on the assumption that NPs are placed randomly in a simulation window such that the NP can come into limited contact with each other. They can also intersect with flanking electrodes. This assumption of material composition can result in microstructures that have NP chains which provide an uninterrupted path from the anode to the cathode

of the device (i.e. a percolating configuration). In the other extreme, there are configurations that have interrupted NP paths that are broken by the dielectric host (i.e. non-percolating configurations). Electrically, these two configurations can lead to notably different values for the properties of composite materials (e.g. effective permittivity and effective breakdown field strength). Scatter plots, along with the 3σ variations, of the effective permittivity, effective breakdown field strength, normalized average electric field, and the energy density illustrate how the variability of the electrical properties can change with the NP volume fraction and with variations in microstructure (Figures 6-9). In addition, Figure 10 illustrates the 3σ variations for each of these properties as well.

5 CONCLUSIONS

Both the maximum energy and the inherent fluctuations within NP composites are important to understand for their

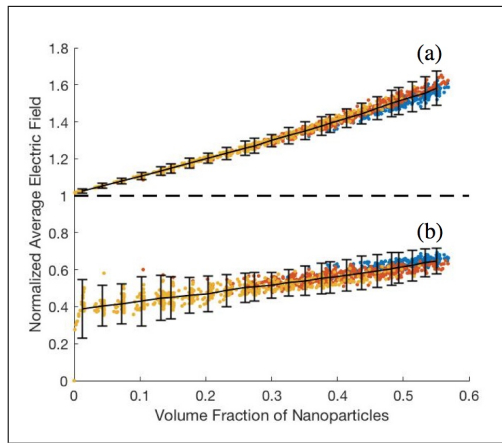


Figure 8: Average electric field within (a) the host material and (b) the nanoparticles, normalized to the electric field of an equivalent capacitor with no nanoparticle inclusions, which is the applied voltage divided by the sample thickness (marked with a dashed line).

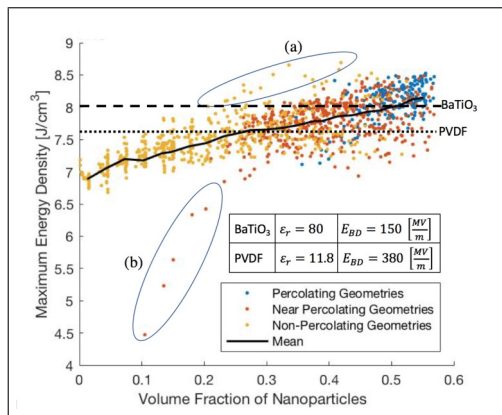


Figure 9: Scatter plot of maximum energy density of simulated geometries with respect to volume fraction. Regions containing (a) best simulated cases and (b) worst simulated cases are indicated. The average values are represented by the solid black line.

potential applications. For energy density, the best case microstructures in this analysis appear to be specific non-percolating configurations between 20% and 40% volume fraction. These are some of the highest volume fraction geometries that still classify as “non-percolating” as seen in Figure 9(a), and these geometries show an increase in energy density of around 14% over an equivalent geometry with no NP inclusions (i.e. pure PVDF). Conversely, several worst cases emerged (Figure 9(b)), wherein the energy density sees a reduction of up to 68% over pure PVDF. This illustrates the wide range of possible microstructures, as well as their potentially large effects on their resulting energy densities. For example, even though high energy densities occur in a range of volume fractions between 20% and 40%, the resulting energy densities can vary up to 1.83 [J/cm³], which is almost 21% of the maximum energy density found in this work.

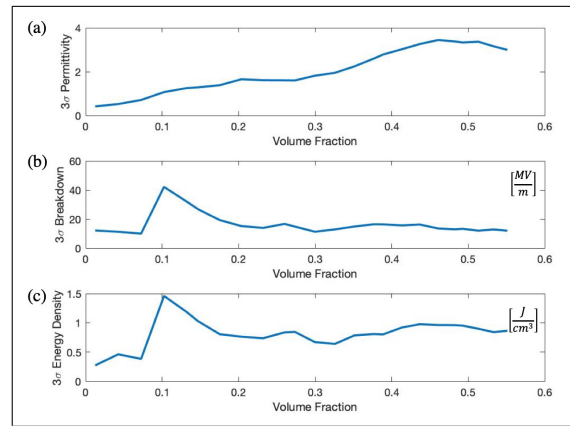


Figure 10: Plots of the 3σ variations at each volume fraction for (a) permittivity, (b) breakdown field strength, and (c) volumetric energy density.

ACKNOWLEDGEMENT

This research was supported in part through research cyberinfrastructure resources and services provided by the Partnership for an Advanced Computing Environment (PACE) at the Georgia Institute of Technology, Atlanta, Georgia, USA.

REFERENCES

- [1] P. Kim et al., “High energy density nanocomposites based on surface- modified BaTiO₃ and a ferroelectric polymer,” *ACS Nano*, vol. 3, no. 9, pp. 2581-2592, 2009.
- [2] J. Y. Li, L. Zhang, S. Ducharme, “Electrical Energy Density of Nanocomposites,” *Applied Physics Letters*, 90, 132901, 2007.
- [3] J. A. Davis, “Energy Density Limits of Multiphase Composites With Dielectric Nanoparticles,” *IEEE Nanotechnology*, vol. 17, no. 2, pp. 250-260, Mar 2018.
- [4] J.A. Davis, D. Brown, W. Henderson, “Impact of Microstructure on Dielectric Nanocomposites with High-k Interfacial Layers,” *IEEE Transactions on Nanotechnology*, vol. 14, no. 4, pp. 717-725, July 2015.
- [5] J.A. Davis, D. Brown, W. Henderson, “Fractal Electrode Formation in Metal-Insulator Composites Near the Percolation Threshold,” *IEEE Transactions on nanotechnology*, vol 12, no. 5, pp. 725-733, Sep. 2013.
- [6] Y. Jin, N. Xia, R. A. Gerhardt, “Enhanced dielectric properties of polymer matrix composites with BaTiO₃ and MWCNT hybrid fillers using simple phase separation.” *Nano Energy*, vol. 30, pp. 407416, 2016.
- [7] X. Zhao et al., “Three-dimensional simulations of complex dielectric properties of random composites by finite element method,” *Journal of Applied Physics*, vol. 95, no. 12, pp. 81108117, Jun. 2004.
- [8] H. Nalwa, “Handbook of Low and High Dielectric Constant Materials and Their Applications,” Academic Press: London, UK, 1999.